



# **A notched connection for CLT-concrete composite slabs resisting to uplift without metallic connectors: experimental investigation**

Vanthet Ouch, Piseth Heng, Quang Huy Nguyen, Hugues Somja, Thierry  
Soquet

## **► To cite this version:**

Vanthet Ouch, Piseth Heng, Quang Huy Nguyen, Hugues Somja, Thierry Soquet. A notched connection for CLT-concrete composite slabs resisting to uplift without metallic connectors: experimental investigation. Fib Symposium 2021: Concrete Structures: New Trends for Eco-Efficiency and Performance, Jun 2021, Lisbon, Portugal. hal-03254979

**HAL Id: hal-03254979**

**<https://univ-rennes.hal.science/hal-03254979>**

Submitted on 9 Jun 2021

**HAL** is a multi-disciplinary open access archive for the deposit and dissemination of scientific research documents, whether they are published or not. The documents may come from teaching and research institutions in France or abroad, or from public or private research centers.

L'archive ouverte pluridisciplinaire **HAL**, est destinée au dépôt et à la diffusion de documents scientifiques de niveau recherche, publiés ou non, émanant des établissements d'enseignement et de recherche français ou étrangers, des laboratoires publics ou privés.

# A notched connection for CLT-concrete composite slabs resisting to uplift without metallic connectors: experimental investigation

Vanthet Ouch<sup>1</sup>, Piseth Heng<sup>2, \*</sup>, Quang-Huy Nguyen<sup>3</sup>, Hugues Somja<sup>4</sup>, Thierry Soquet<sup>5</sup>

1. PhD candidate, Laboratoire de Génie Civil et Génie Mécanique/Structural Engineering Research Group, Institut National des Sciences Appliquées de Rennes, Rennes, France.
2. Research engineer, Laboratoire de Génie Civil et Génie Mécanique/Structural Engineering Research Group, Institut National des Sciences Appliquées de Rennes, Rennes, France.
3. Associate Professor, Laboratoire de Génie Civil et Génie Mécanique/Structural Engineering Research Group, Institut National des Sciences Appliquées de Rennes, Rennes, France.
4. Professor, Laboratoire de Génie Civil et Génie Mécanique/Structural Engineering Research Group, Institut National des Sciences Appliquées de Rennes, Rennes, France.
5. Architect, Architecture Plurielle agency, Rennes, France

\*Corresponding author email: piseth.heng@insa-rennes.fr

## Abstract

In search for a solution of a sustainable construction with less impact on environment while maintaining a sufficient structural performance, CLT-concrete composite slabs/beams have been increasingly proposed for medium-to-large span structures. Different types of mechanical shear connectors have been studied in the literature for these composite elements. Among them, the notch type is the most preferable due to the high shear resistance contributed by the concrete. However, steel screw or bolt is needed in the connector to limit the uplift between the timber and the concrete. In this paper, a novel type of notched connectors with a particular shape that is able to limit the uplift without the need for steel bolts is proposed. The main objective of this paper is to determine the local and global behaviours of this new shear connector by experimental investigations. Two series of experimental tests were ordered by Thierry Soquet, an architect of Architecture Plurielle and an inventor of innovative construction systems directed by Horizon Bois. A series of three symmetrical push-out tests were performed on large-scale specimens in order to determine the shear resistance, the stiffness, the deformation capacity and the failure mode of the connector. The test results have shown high shear resistance and large stiffness of the connectors. However, the ductility of the connectors is still limited, as the failure mode was governed by the shear failure of the transverse layer of the CLT. In addition, the global behaviour of the CLT-concrete slab was assessed by a series of two full-scaled flexural tests on the slab specimens under a positive bending moment. It was shown in the test results that the design of the composite slab was not limited by the flexural bearing capacity as a high value of the maximum bending moment was obtained in the tests, but governed by the deflection of the composite slab. The delay in the tests caused by the Covid crisis has moreover set in evidence the importance of the shrinkage of concrete in the total deflection.

**Keywords:** *Shear notch connectors, CLT-concrete composite slabs, Push-out tests, Flexural tests, Uplift.*

## 1. Introduction

The high amount of carbon dioxide released to atmosphere creates serious drawbacks for concrete and steel structures. This brings back the interests of using the timber in the construction on account of environmental sustainability along with a sufficient structural performance. Timber-concrete composite members have been increasingly studied for medium-to-large span structures (e.g. (Deam et al., 2008), (Lukaszewska et al., 2008), (Jiang and Crocetti, 2019)). The global behaviour of these composite structures depends largely on the connection between the two materials. An efficient connection must ensure the transfer of shear forces between the concrete and the timber with limited slips and uplifts. Different types of mechanical shear connectors of the timber-concrete composite elements have been

studied in the literature. A detailed review of these connectors is given by (Yeoh et al., 2011). Among them, the notch type is the most preferable in terms of high shear resistance. However, steel screws or bolts are needed in the connector to limit the uplift between the timber and the concrete, which requires tools and skills and slows down the construction process. Thierry Soquet, an architect of the Architecture Plurielle agency and a designer of the Horizons Bois building in Rennes, in collaboration with INSA Rennes developed a novel notched connector for a CLT-concrete composite slab with a particular form that is able to limit the uplift between the concrete and the CLT panels without the need for screws or bolts.

This paper presents the experimental study on the effectiveness of the proposed notched connector used in CLT-concrete composite floors by a series of three symmetrical push-out tests and two large-scale four-point bending tests.

## 2. Push-out tests

For the characterisation of a shear connection between composite members, the standard push-out test is commonly used. In this paper, symmetrical large-scale push-out tests were conducted to study the behaviour of the novel notched connection of the CLT-concrete composite slab.

### 2.1. Test setup

The test setup was made to conform to the push-out test given in Annex B of Eurocode 4 part 1-1 (2004) and EN 26891 (1991), with an adaptation to fit with the configuration of the CLT-concrete composite slab. Illustrated in Figure 1, the test setup consisted of a force jack with a capacity of 1500 kN, a loading HEB-300 steel piece, a specimen of the CLT-concrete connection and a supporting steel table. In the test setup, the specimen was placed vertically on the supporting table. The force jack applied a uniform vertical load on the top surface of the CLT block of the specimen via the HEB-300 profile while the supporting steel table provided a reaction to the reinforced concrete panels. The width of the profile (300 mm) almost covered the width of the CLT panel (330 mm) and spanned over to the concrete notches so that the loading could be as uniform as possible. In order to avoid a dangerous collapse of the specimen, four steel angles placed around the four faces of the specimen were fixed on top of the supporting steel plate by 150-mm welds in the centre of the angle. These angles were however not in contact with the specimen.

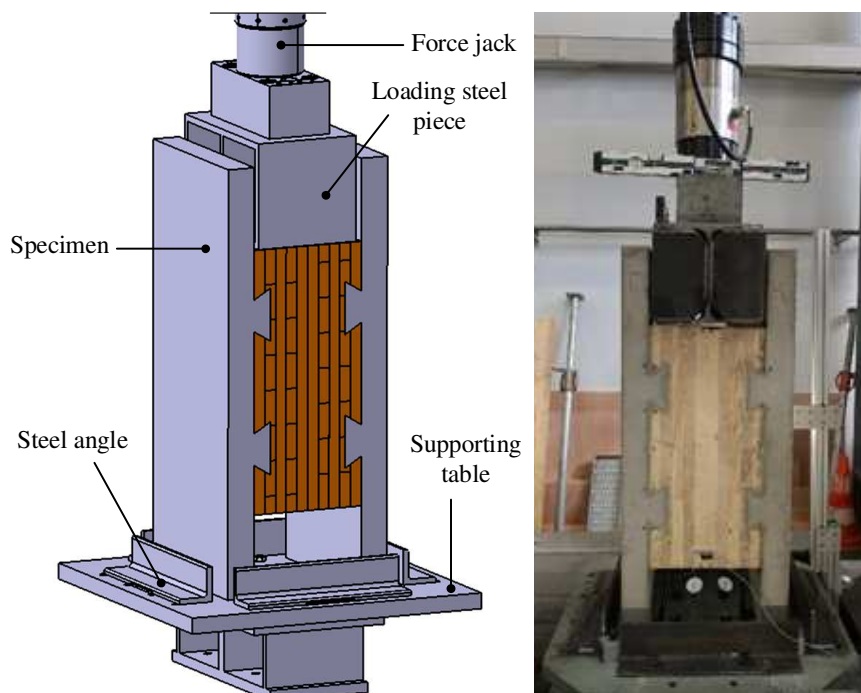


Figure 1. Pushout test: Description of test configuration.

## 2.2. Test specimen

Three specimens (namely B1, B2 and B3) were fabricated. Each specimen was composed of two CLT panels glued to each other and placed between two reinforced concrete panels (Figure 2a). Each RC panel was connected to the CLT panel by two notched connectors. The notch connector (Figure 2b) was obtained by cutting a notch from the CLT panel. A U-shape rebar cage was put in it (Figure 2c). In the fabrication process, the concrete was casted on each CLT panel separately using the same concrete on the same day. The concrete was casted directly on the CLT panel during the fabrication of the specimen without laying plastic films nor applying any paint. After the concrete was cured, the two pieces were glued to each other at the free surface of the CLT panels (Figure 2a) using polyurethane glue. This process avoids the inconvenience of casting concrete at a different time for each concrete panel.

The dimensions of the specimens are given in Figure 3. Specimen B1 has a width of  $b = 500$  mm whereas specimens B2 and B3 have a width of  $b = 400$  mm. Reinforcement mesh ST15 was also placed inside the concrete panel.

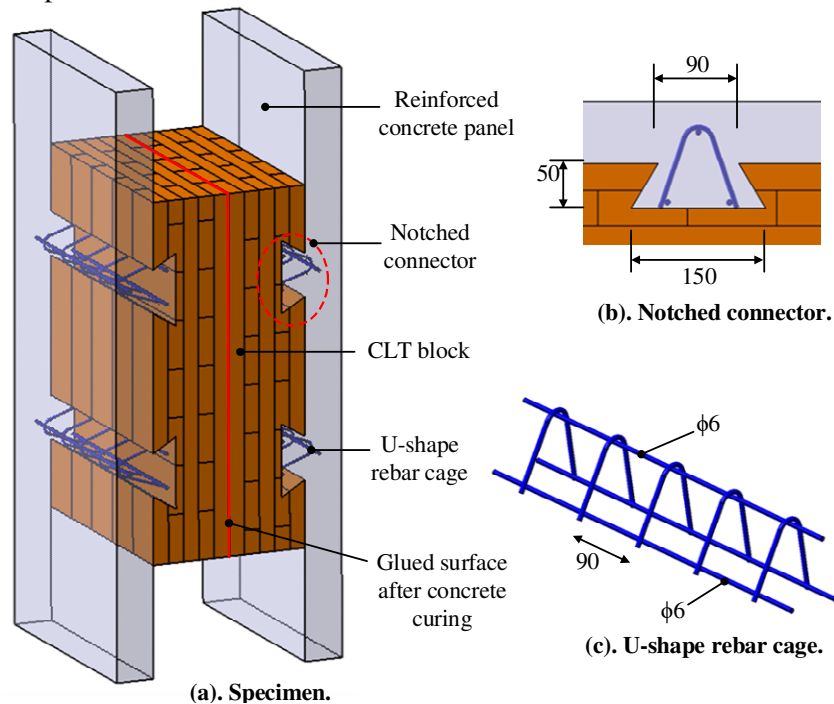


Figure 2. Pushout test: Description of test specimen (dimensions in mm).

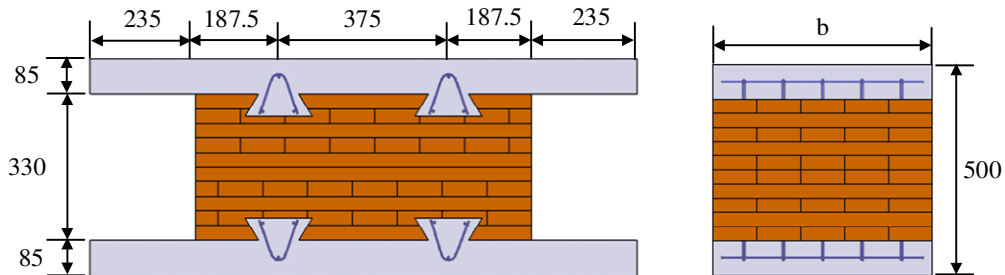


Figure 3. Pushout test: Dimension of the specimen (dimensions in mm).

## 2.3. Material properties

According to Annex B of Eurocode 4 part 1-1 (2004), for a preparation of the specimen in the standard push-out test, the compressive strength of the concrete at the time of testing should be  $70\% \pm 10\%$  of the specified strength of the concrete. In order to achieve this objective, the concrete at young age was used. Based on the expressions in Eurocode 2 part 1-1 (1992) for determining the concrete strength in relation to the age of concrete, the concrete compressive strength at the age between 7 and 14 days reaches a value between 68% and 85% of the strength at 28 days.

The concrete panel had a concrete strength class of C35/40 formulated according to the norm EN 206-1, having the class of environment XF1. 2 series of three cylinder specimens with a dimension of 11×22cm were tested on the day of each push-out test using standard compressive tests for compressive strength and using Brazilian tests for tensile strength. The results are reported in Table 1.  $f_{ct}$  and  $f_{ctm}$  are tensile strength of each specimen and their mean value, respectively.  $f_c$  and  $f_{cm}$  are compressive strength of each specimen and their mean value, respectively.

Table 1. Pushout tests: Concrete strength.

Test	Age (days)	$f_{ct}$ [MPa]	$f_{ctm}$ [MPa]	$f_c$ [MPa]	$f_{cm}$ [MPa]
B1	6	3.16	3.20	33.82	34.51
		3.50		34.46	
		2.94		35.25	
B2	3	2.80	2.56	29.31	29.12
		2.35		28.70	
		2.53		29.36	
B3	7	3.72	3.39	39.73	39.51
		3.21		38.95	
		3.23		39.84	

The CLT panel was made of massive wooden boards with a minimum class of C18 and a mean density of 420 kg/m<sup>3</sup> specified in the technical specification of the product (TOT'm X, 2020). The steel rebars have a steel grade of BST 500 S.

## 2.4. Instrumentation and test procedure

The compressive load, applied to the CLT panel by the force jack, was transferred to the concrete panels through concrete notches. This force was then balanced by the reaction forces provided by the supporting table.

In order to measure relative displacements between the CLT and concrete panels (slips and uplifts), the measurement using Digital Image Correlation method was adopted. In this method, a series of photos were captured during the course of the test at each increment of loading by two high resolution cameras (one at the front and the other at the back surface of the specimen). These photos were then used to employ tracking and image registration measurements of changes in the images over time. The precision determined for this test was currently  $\pm 0.1$  mm. Points were marked on the concrete and the CLT panels (see Figure 4); the change of the positions of these points was tracked and measured in order to compute the slips and uplifts.

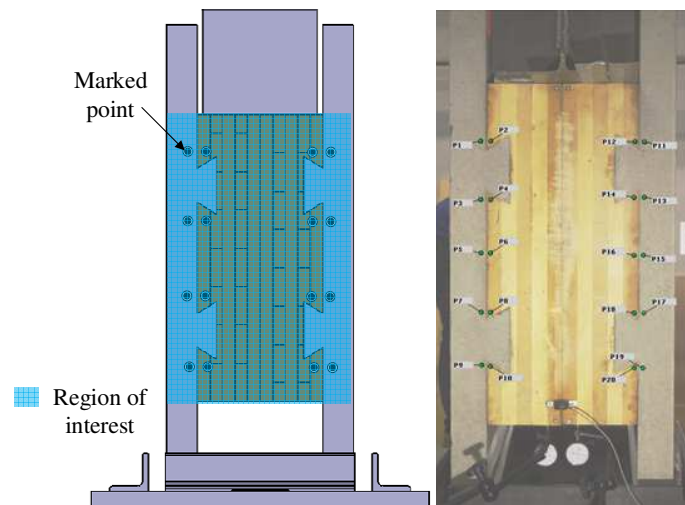


Figure 4. Pushout test: Zones for Digital Image Correlation method.

The load was applied according to the test procedure described in Annex B of Eurocode 4 part 1-1 (2004). With a loading rate of 1 mm/min, 25 loading/unloading cycles between 40 % and 5 % of the expected failure load were initially applied to the specimen in order to remove the friction between the concrete and CLT surfaces. The load was then monotonically increased up to failure with a loading rate of 1 mm/min. The expected failure load was (under)estimated at 400 kN for the test B1 while it was updated to 650 kN for tests B2 and B3.

## 2.5. Results

Figure 5 shows the evolution of the force in function of the elongation of the force jack for the three tests. The maximum loads obtained for tests B1, B2 and B3 are 840 kN, 685 kN and 690 kN, respectively. In all the three tests, the failure mode was governed by a brittle shear rupture of one of the weak layers of the CLT panel, as shown in Figure 6.

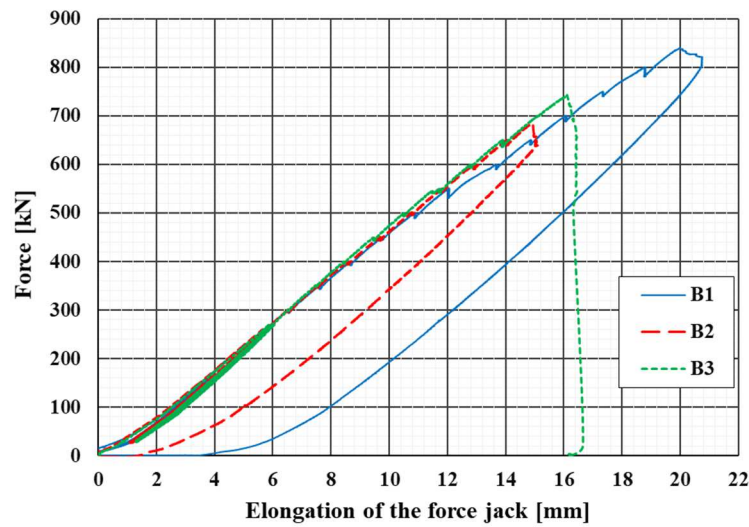


Figure 5. Pushout test: Force-elongation curve of the force jack.

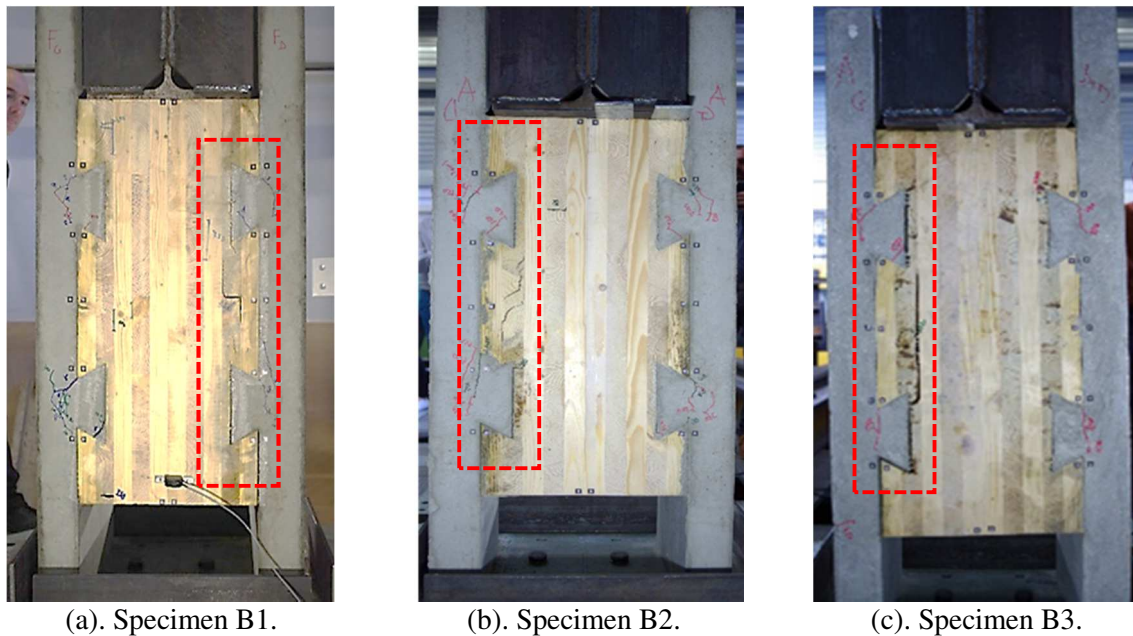


Figure 6. Pushout test: Shear rupture of one of weak layers of the CLT panel.

Figure 7 illustrates the evolution of the mean slips and the mean uplifts in function of the force per connector per meter width. The maximum value obtained from the three tests ranges between 0.8 mm and 1.6 mm for the slip and between 0.7 mm and 1 mm for the uplift. The maximum load attained per connector per meter width ( $F_{max}$ ) is 419 kN, 421 and 461 kN for test B1, B2 and B3, respectively. The



mean value ( $\mu$ ) and the standard deviation ( $\sigma$ ) of the maximum load for the three tests are 434 kN and 24 kN. The corresponding mean slips to the maximum force ( $\delta_{F_{max}}$ ) are 0.79 mm, 1.02 mm and 0.9 mm, respectively. The corresponding mean uplifts to the maximum force ( $u_{F_{max}}$ ) are 0.57 mm, 0.67 mm and 0.59 mm, respectively.

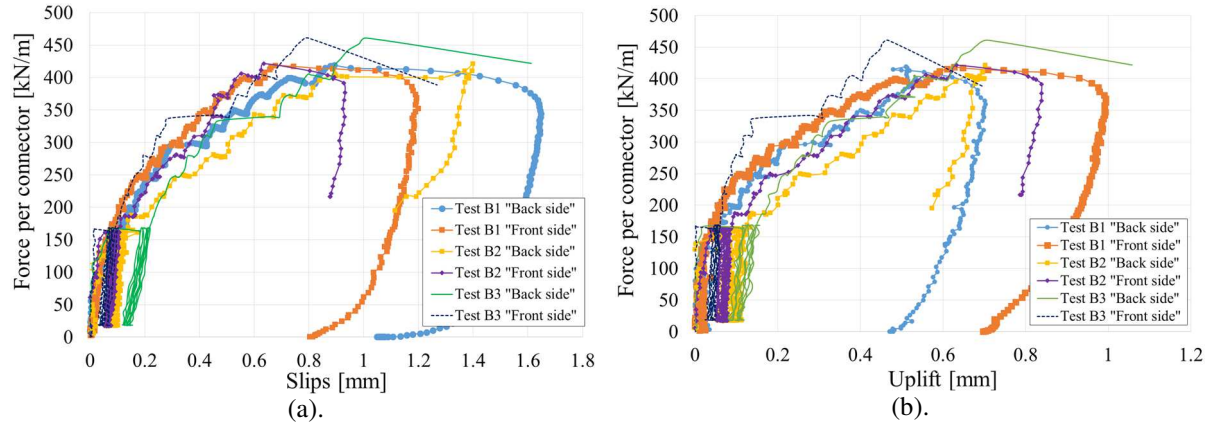


Figure 7. Pushout test: (a). Force per connector versus slips. (b). Force per connector versus uplifts.

While the strength of the connector is defined by the maximum load applied at failure ( $F_{max}$ ), the stiffness is quantified by slip modulus at different load levels. Based on the model proposed by (Ceccotti, 1995), the stiffness at service limit state ( $K_{ser}$ ) is determined by a secant slope of a straight line that connects the beginning of the load-slip curve to a point at 40 percent of the failure load. The stiffness at ultimate limit state ( $K_u$ ) is computed as equal to  $\frac{2}{3}K_{ser}$ . The computation of these stiffness is reported in Table 2.

Table 2. Shear strength and slip moduli values for one connector per one meter width.

Test	$F_{max}$ [kN/m]			$\delta_{F_{max}}$ [mm]	$u_{F_{max}}$ [mm]	$K_{ser}$ [kN/m/m]			$K_u$ [kN/m/m]		
		$\mu$	$\sigma$				$\mu$	$\sigma$		$\mu$	$\sigma$
B1	419	434	24	0.79	0.57	$1.81 \times 10^6$	$1.49 \times 10^6$	$0.28 \times 10^6$	$1.20 \times 10^6$	$1.00 \times 10^6$	$0.18 \times 10^6$
B2	421			1.02	0.67	$1.38 \times 10^6$			$0.92 \times 10^6$		
B3	461			0.90	0.59	$1.29 \times 10^6$			$0.87 \times 10^6$		

### 3. Flexural tests

Four-point bending tests were applied to two large-scale specimens of the CLT-composite slab with the new notched connectors in order to validate the functioning of the connectors in real configuration, and measure the global structural response.

#### 3.1. Specimen and test setup

Two slab specimen were fabricated. Each specimen had a dimension of 3200×6710×245mm and was composed of a CLT panel with a thickness of 165 mm connected to a reinforced concrete panel with a thickness of 85 mm by a series of 13 notched connectors (Figure 8).

The test setup consisted of a slab specimen, two supports, a force jack with a capacity of 1500 kN and a loading system to apply a four-point loading configuration (Figure 9a). In this test setup, the specimen was simply supported. It was placed on two support systems, and the load was applied vertically from the force jack onto the specimen through the loading system. The support 1 (conceptualized for supporting walls) was a linear support that gave supporting contacts to the entire width of the specimen (Figure 9b). At this support, the horizontal displacement of the CLT panel was restrained by the profile UPN 300. In test F1, the support condition was applied to fit with an actual condition, in which two point supports (conceptualized for supporting columns) placed at corners below the specimen were used

for the support 2 (Figure 9c). PTFE layers were used in order to minimize the friction between the support and the CLT panel. Due to a premature shear failure of the specimen at the point supports in test F1, a linear support (Figure 9d) was adopted for the support 2 in test F2. The span between the supports and the loading positions are given in Figure 10.

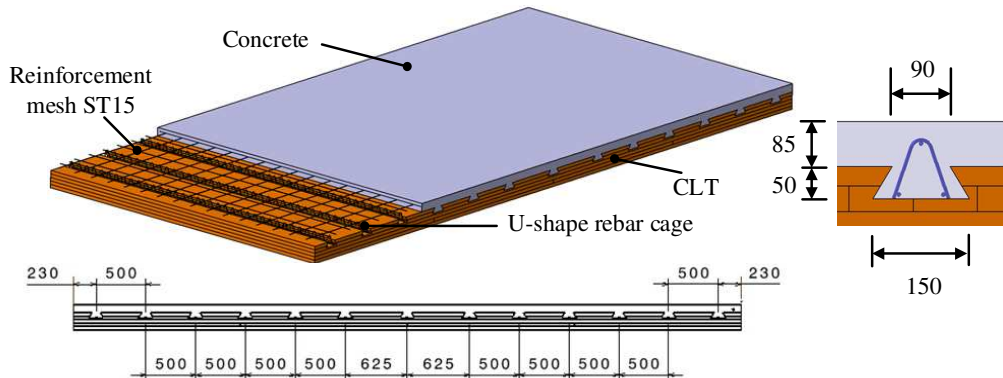


Figure 8. Flexural test: Description and dimensions of test specimen (dimensions in mm).

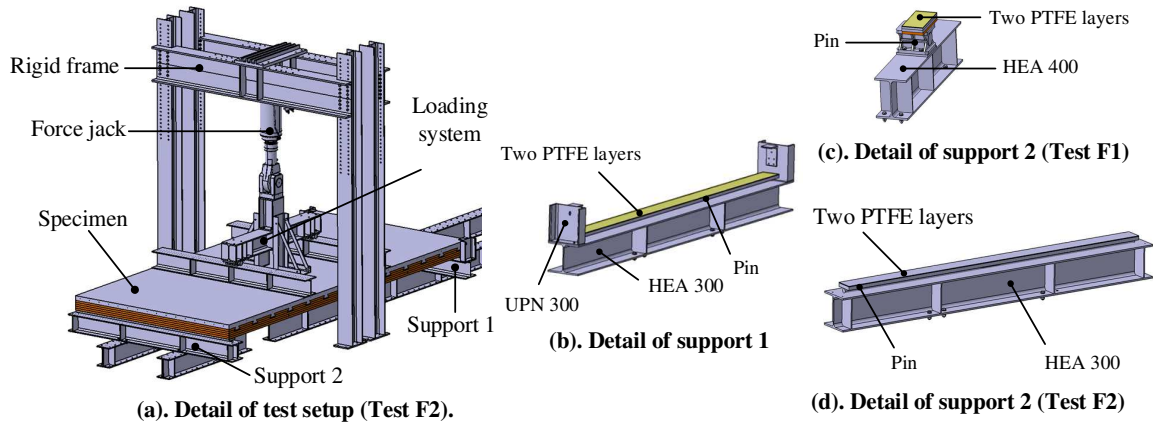


Figure 9. Flexural test: Description of test configuration.

### 3.2. Material properties

The same concrete class for concrete panels and the same wood class for the CLT panels as in pushout tests were used. Three cylinder specimens with a dimension of 11×22cm were tested on the day of each flexural test for concrete strength and reported in Table 3.

Table 3. Flexural tests: Concrete strength.

Test	Age (days)	$f_c$ [MPa]	$f_{cm}$ [MPa]
F1	120	56.45	56.60
		56.33	
		57.01	
F2	147	56.61	55.35
		53.25	
		56.18	

### 3.3. Instrumentation and loading procedure

The force generated by the hydraulic force jack was measured by an integrated double force sensors ( $\pm 500$  kN and  $\pm 1500$  kN). The slips between the CLT and the concrete panels were determined by 8 LVDT sensors (4 at each side along the specimen) noted by CG1 to CG8 with a capacity of  $\pm 2.5$  mm. Four LVDT sensors with a capacity of 25 mm (CD1 to CD4) were positioned below the specimen close



to the support to measure the settlement of supports for a displacement correction when computing the deflection. The positions of the sensors are given in Figure 10.

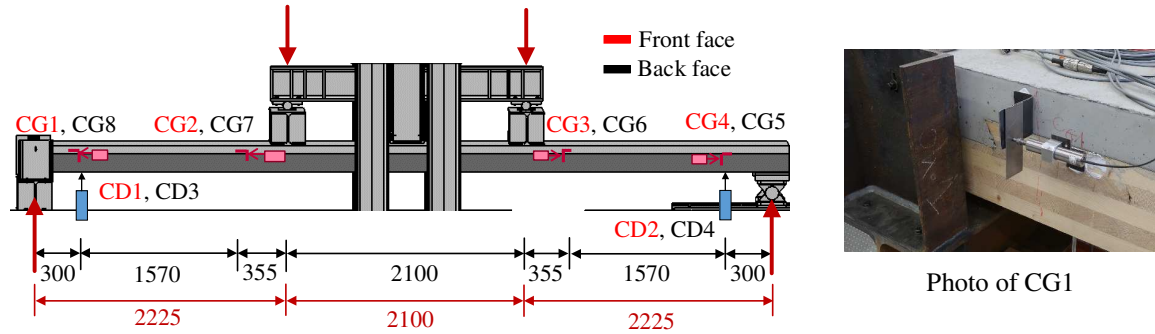


Figure 10. Flexural test: Positions of sensors LVDT (dimensions in mm).

Apart from the analogue sensors, three high resolution photo cameras were also installed for an analysis using digital image correlation technology (DIC). The deflection of the specimen was determined by recording the evolution of points on steel board fixed below the CLT at mid width (noted by C1 to C5). The slips (G1 and G2) and the uplifts (D1 and D2) were obtained from points on the recording areas. The measuring positions of the areas for the DIC are presented Figure 11.

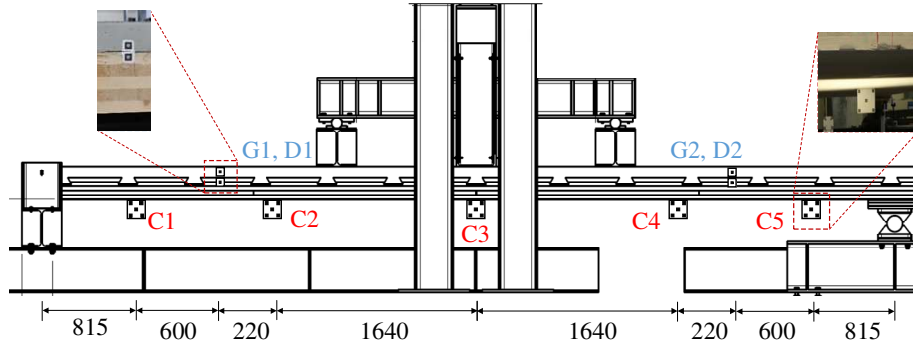


Figure 11. Areas for the DIC (dimensions in mm).

Regarding the loading procedure, 25 initial loading/unloading cycles between 40 % and 5 % of the estimated failure load was applied to the specimen in order to remove the friction with a loading rate of 1 mm/min. The failure load is estimated at 403 kN. One more cycle at the estimated ultimate limit state was then performed before it was monotonically increased up to failure with a loading rate of 1 mm/min.

### 3.4. Influence of shrinkage effects on the deflection

The first flexural test (F1) was performed four months after the concrete casting of the specimen. This delay was due to the first period of lockdown imposed by the French government during the Covid-19 crisis. During storage, many concrete cracks (see Figure 12) were observed on the concrete panel of the specimen, which brought to light the suspicion of non-negligible effects of concrete shrinkage on the deflection. However, it was not possible to quantify the deflection caused by this effect.

It was decided later to measure the evolution of the deflection of the specimen F2 during around three months. The specimen was placed on the supports of the flexural test configuration with only the self-weight of the specimen applied on it. Laser sensor was installed at the mid-span below the specimen in order to measure the deflection over time. The specimen F2 was casted with an initial positive deflection at the mid-span of 19 mm. Figure 13 shows the evolution of the mid-span deflection over time. The deflection contributed by the shrinkage for 100 days can be vastly computed at 16 mm, being the difference between the deflections at the time of 100 days and of 0 day. This value is not negligible and calls for further investigation through a dedicated experimental campaign.

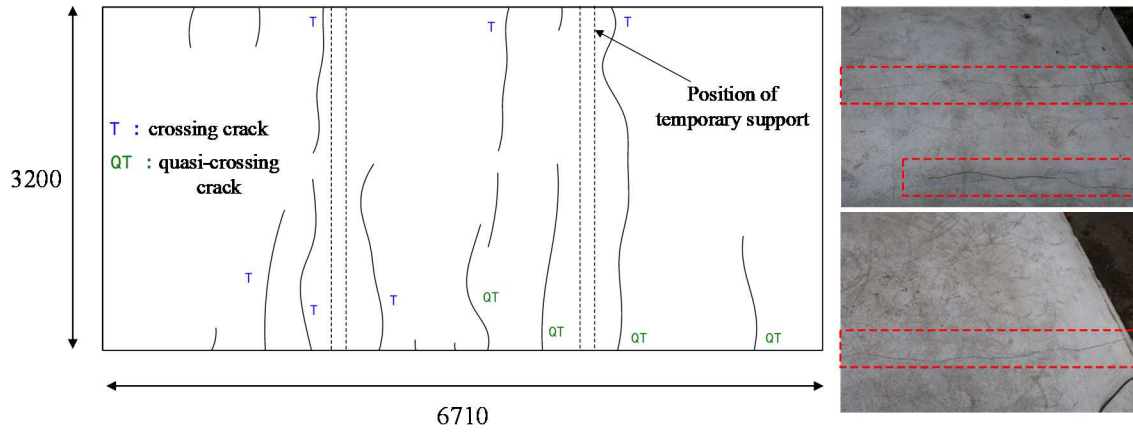


Figure 12. Specimen F1: Cracks due to shrinkage effects (dimensions in mm).

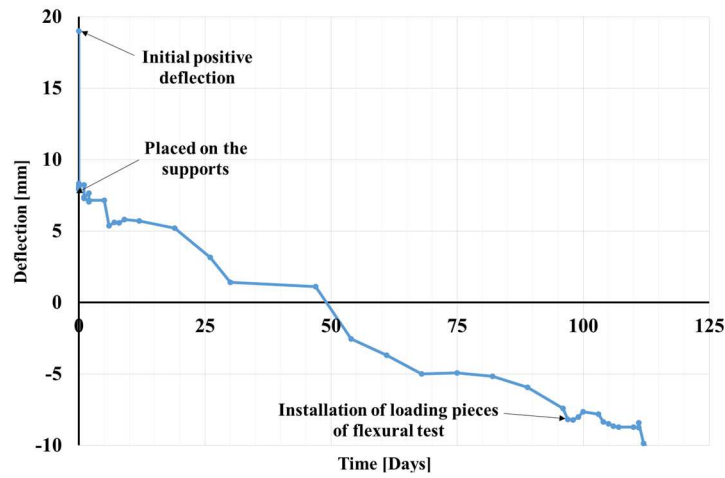


Figure 13. Specimen F2: Evolution of mid-span deflection over time.

### 3.5. Results of flexural tests

Figure 14 illustrates the envelop curves of the elongation evolution of the force jack and of the mid-span deflection in function of the force for both tests. The maximum force obtained for test F1 is 590 kN, corresponding to a maximum mid-span deflection of 71.40 mm. The failure mode of Test F1 was governed by a shear rupture of the concrete panel close to the point supports (Figure 15a). On the other hand, in the second test, the loading was stopped at 725 kN for security reasons when many wood layers were ruptured (Figure 15b). This was to avoid a brittle collapse of the system, as the failure seemed to be governed by the rupture of the CLT layers in tension. In addition, a large mid-span deflection of the specimen of 93 mm was already obtained (Figure 14b).

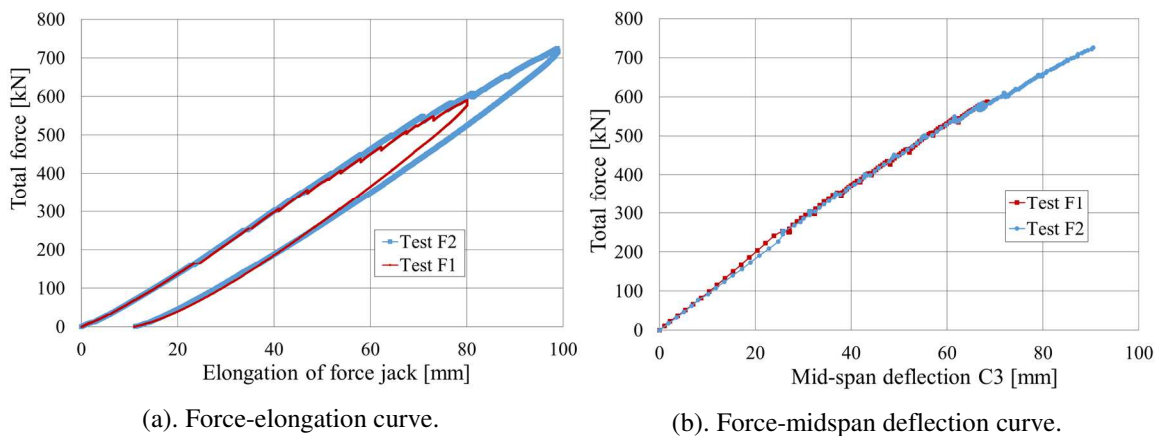


Figure 14. Flexural tests: Evolution of the elongation of the force jack and the mid-span deflection.

Figure 16 represents the evolution of the slips in function of the force for both tests. The maximum slips obtained for tests F1 and F2 are 2.38 mm and 0.66 mm, respectively. The large values of the slips measured by sensors CG4 and CG5 in test F1 were relative displacements caused by shear cracks near the point supports (Figure 15a). Due to the errors in the interpretation of the DIC of G1, G2, D1 and D2 for test F1, the results are not presented here. The evolution of the uplifts by D1 and D2 for test F2 is described in Figure 17. The maximum mean uplift obtained for test F2 is 0.43 mm. It can be concluded from these results that in both tests the global response of the specimens were almost linear until the failure of the specimens.

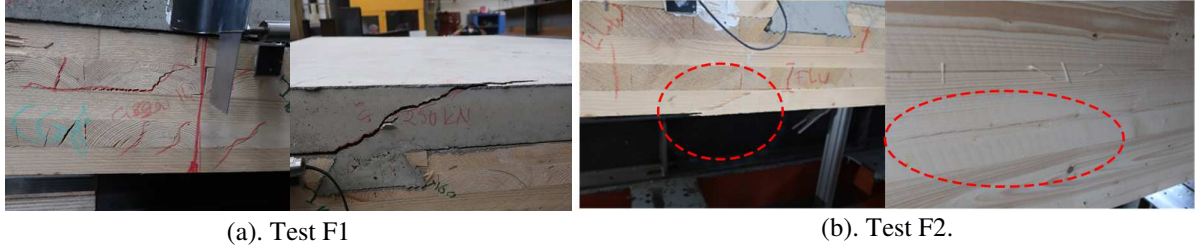


Figure 15. Flexural tests: Failure of the specimen.

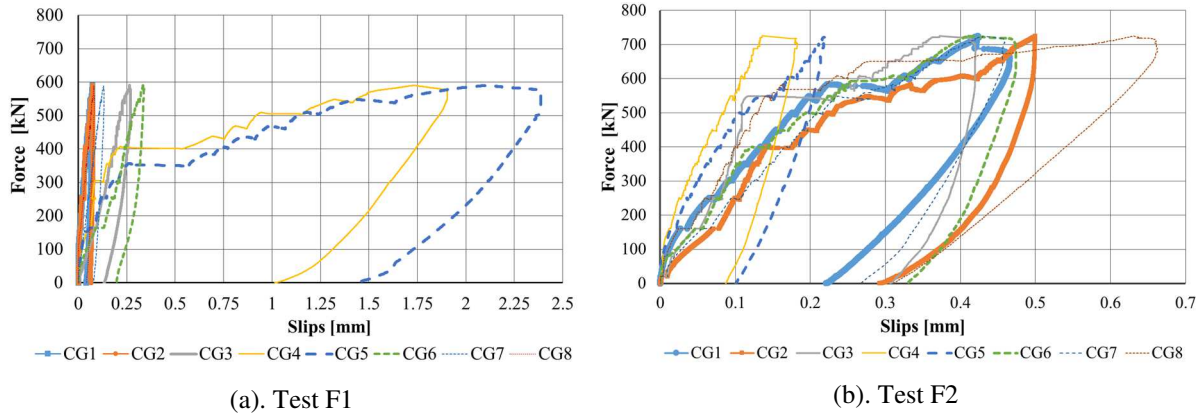


Figure 16. Flexural tests: Evolution of slips in function of force.

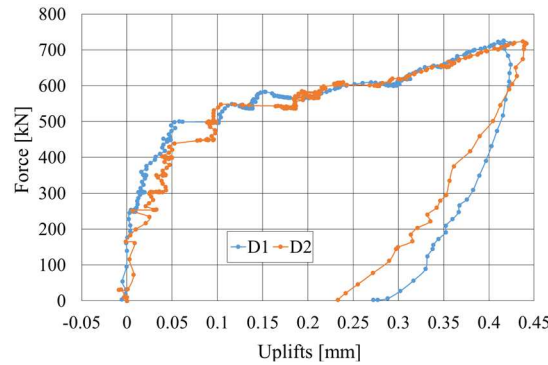


Figure 17. Flexural tests: Evolution of uplifts in function of force for test F2.

### 3.6. Verification of deflection of the specimen

A simplified calculation method or “gamma method” provided in Annex B of Eurocode 5 – part 1-1, is usually adopted for the design of timber-concrete composite floors. (Jiang and Crocetti, 2019) proposed a modification of the gamma method to apply to CLT-concrete composite floor with 5-layer CLT panel. It is interesting to verify the accuracy of this method to predict the flexural stiffness of the present CLT-concrete composite floor with the novel notched connectors. The flexural stiffness at SLS and ULS are computed with the modified gamma method using the mean value of  $K_{ser}$  and  $K_u$  provided in Table 2. As illustrated in Figure 18, the gamma method predicts well the flexural stiffness of the present CLT-concrete composite floor with the new notched connectors. Load levels corresponding to a load combination for SLS and for ULS as indicated in Eurocode 2 (1992) are also given in the figure. In fact,

the wood-concrete connection is very stiff compared to the effect of rolling shear within the CLT panel. It can also be seen that a small difference is obtained for the flexural stiffness when using  $K_{ser}$  and  $K_u$ .

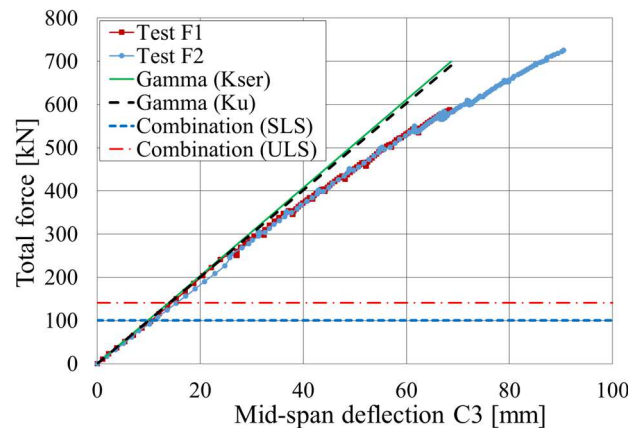


Figure 18. Flexural tests: comparison of force-deflection responses.

It is clear that the resistance of the composite floor is sufficient for the ultimate limit state design. However, with the influence of the shrinkage effects, it is needed for a service limit state verification.

## 4. Conclusion

This paper presents an experimental investigation on the behaviour of the CLT-concrete composite floor with novel notched connectors. Three symmetrical push-out tests and two full-scale four-point flexural tests were carried out in order to validate the effectiveness of the proposed notched connector in the CLT-concrete composite floor. The failure mode of all the specimens in the push-out tests was governed by the shear rupture of the weak layer of the CLT panel. The push-out test results showed high values of the shear strength and of the stiffness although low ductility was obtained. The results of the flexural tests showed the efficiency of the notched connector, as the failure mode of the specimen in test F2 was governed by the rupture of the tensile layers of the CLT, and the maximum slips and uplifts were smaller than the ultimate values obtained in the pushout tests. The modified gamma method (Jiang and Crocetti, 2019) provided a good agreement of the flexural stiffness with the experimental result. In addition, a small difference of the flexural stiffness is obtained when using the value of the stiffness  $K_{ser}$  and that of  $K_u$  in the gamma method. At last, while a high bending resistance of the composite floor was obtained, the evolution of the deflection caused by the shrinkage effects requires further investigations as the deflection verification at service limit state is critical.

## References

- Deam, B.L., Fragiocomo, M., Buchanan, A.H., (2008). Connections for composite concrete slab and LVL flooring systems. *Materials and Structures*, 41(3), 495-507.
- Lukaszewska, E., Johnsson, H., Fragiocomo, M., (2008). Performance of connections for prefabricated timber-concrete composite floors. *Materials and structures*, 41(9), 1533-1550.
- Jiang, Y., Crocetti, R., (2019). CLT-concrete composite floors with notched shear connectors. *Construction and Building Materials*, 195, 127-139.
- Yeoh, D., Fragiocomo, M., De Franceschi, M., Heng Boon, K., (2011). State of the art on timber-concrete composite structures: Literature review. *Journal of structural engineering*, 137(10), 1085-1095.
- CEN EN 1994, part 1-1 (2004). Eurocode 4: Design of composite steel and concrete structures. Part 1-1: General rules and rules for buildings". Brussels, Belgium.
- CEN. ISO EN 26891 (1991). Timber structures – joints made with mechanical fasteners general principles for the determination of strength and deformation characteristics. In ISO (Ed.), ISO EN 26891. Brussels: CEN.
- CEN EN 1992, part 1-1 (1992). Eurocode 2: Design of concrete structures. Part 1-1: General rules for buildings.
- Avis Technique TOT'm X (2020): [https://evaluation.cstb.fr/fr/avis-technique/detail/3.3-17-925\\_v2/](https://evaluation.cstb.fr/fr/avis-technique/detail/3.3-17-925_v2/).
- Ceccotti A., (1995). Timber-concrete composite structures. In: Blass HJ, editor. *Timber engineering – STEP 2. Structural Timber Education Programme*. The Netherlands: Centrum Hout; 1995. p. E13/1-E13/12.